J Mol Model (2011) 17:577–585
DOI 10.1007/s00894-010-0743-3

ORIGINAL PAPER

DFT investigation on the reaction mechanism catalyzed by α-phosphomannomutase1 in protonated/deprotonated states

Hui-Ying Chu · Qing-Chuan Zheng · Xue Li · Yong-Shan Zhao · Ji-Long Zhang · Hong-Xing Zhang

Received: 11 July 2009 / Accepted: 4 May 2010 / Published online: 30 May 2010

Abstract Congenital disorder of glycosylation type 1a (CDG-1a) which is a congenital disease, is caused by mutations in α-Phosphomannomutase1. The reaction mechanism of the α-phosphomannomutase1 enzyme has been investigated by means of density functional theory using the hybrid functional B3LYP. The α-phosphomannomutase1 catalyzes the interconversion of the α-D-mannose 1-phosphate to D-mannose 6-phosphate *via* a mannose-1,6-(bis) phosphate intermediate. The quantum chemical models, which were chosen in protonated/deprotonated states models, were built on the basis of the docking result. The process of the phosphoryl group transferred from Asp19 to the mannose 6-phosphate is in different steps in the two states, but are both coupled with the protons transfer. Our computational results support the hypothesis that the Asp19 as a nucleophile plays an important role in the α-phosphomannomutase1 biology function, and indicate Gln62 could help to stabilize the phosphoryl group and the structure of the substrate. In addition, we can conjecture that the deprotonated state is more suitable for product release.

Keywords α-Phosphomannomutase1 · Density functional theory · Molecular dynamics · Reaction pathway

H.-Y. Chu · Q.-C. Zheng · X. Li · Y.-S. Zhao · J.-L. Zhang · H.-X. Zhang (✉)
State Key Laboratory of Theoretical and Computational Chemistry, Institute of Theoretical Chemistry, Jilin University, Changchun 130023, People's Republic of China
e-mail: zhanghx@mail.jlu.edu.cn

H.-Y. Chu
State Key Laboratory of Molecular Reaction Dynamics, Dalian Institute of Chemical Physics, Chinese Academy of Sciences, Dalian 116023, China

Introduction

N-glycosylations occurs in all mammalian cells, and abnormal protein glycoylation affects numerous functions in the organism [1, 2]. In humans, deficiency of the α-phosphomannomutase1 causes congenital disorder of glycosylation type 1a (CDG-1a) [3–5], a broad spectrum disorder with developmental and neurological abnormalities. The classical clinical presentations of a CDG-1a patient include psychomotor delay, ataxia, and variable dysfunction of liver, heart and digestive and coagulation system [1, 6–10].

The α-phosphomannomutase1 catalyzes the interconversion between D-mannose 6-phosphate and α-D-mannose1-phophate (the reaction catalyzed by α-phosphomannomutase1 shown in Scheme1) *via* a bisphosphorylated intermediate, and α-phosphomannomutase1 is required for GDP-mannose and dolichol-phosphate-mannose biosynthesis [11, 12]. The α-phosphomannomutase1 belongs to the haloalkanoic acid dehalogenase superfamily (HADSF), distinguishing it in structurally and mechanistically from the phosphomanno/phosphoglucomutase enzyme of the phosphohexomutase superfamily which are integral to glycolysis in both prokaryotes and eukaryotes [13], and are integral to alginate biosynthesis in Gram-negative bacteria [12, 14].

In 2006, Regni *et al*. [15] have concluded the following catalysis mechanism for phosphomannomutase/phosphoglucomutase of the same superfamily: the reaction entails two phosphoryl groups transfer. The first phosphoryl group transfers from a phosphorylted residue of the enzyme to bound substrate and produces a bisphosphorylated intermediate. The intermediate must then reorient ~180° to be in the position for second phosphoryl group transfers from the intermediate back to the enzyme. Silvaggi *et al*. [12] reported the X-ray crystal structure of α-phosphomannomutase1 (PDB code 2FUC), revealed that the key active-site residue

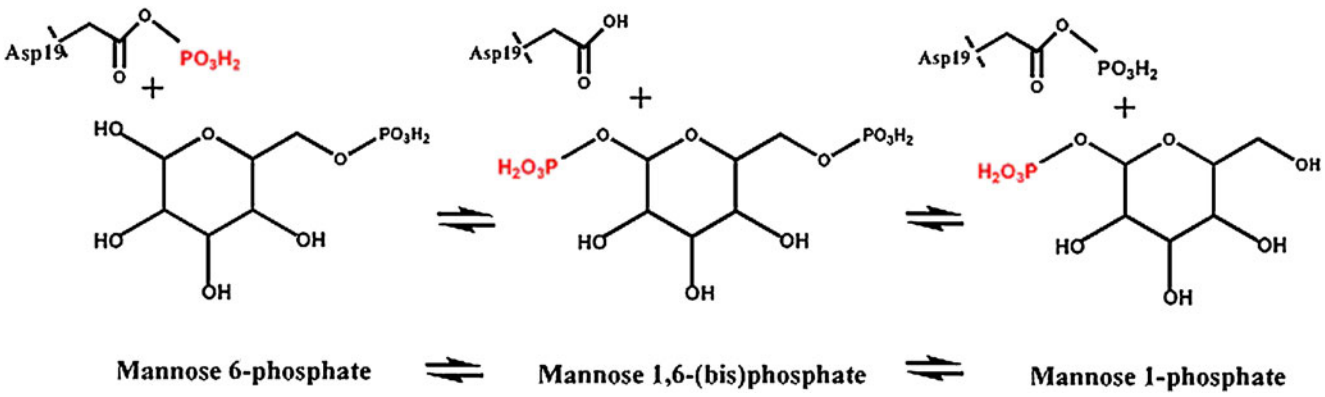

Scheme 1

is catalytic nucleophile Asp19, and proposed the similar reaction mechanism for α-phosphomannomutase1: the interconversion of the α-D-mannose 1-phophate to D-mannose 6-phosphate *via* a mannose-1,6-(bis) phosphate intermediate generated by the α-phosphomannomutase1.

By far, no theoretical studies report has been found about the α-phosphomannomutase1. Although the proposed mechanism is reasonable, there are some questions about the catalysis details which remain unknown. In the present study, quantum chemical models were constructed based on the docking result of α-phosphomannomutase1 with D-mannose 6-phosphate, and the energies of the phosphoryl group in protonated/deprotonated states transfer steps of the proposed mechanism were investigated by using the hybrid density functional theory (DFT) method the three-parameter hybrid exchange functional of Becke and Lee, Yang, and Parr correlation functional (B3LYP), which has been extensively used to study enzyme mechanism in recent years [16–18]. Our results may be helpful to understanding the mechanism of α-phosphomannomutase1 clearly.

Materials and methods

Molecular mechanics, molecular dynamics simulations and docking

Molecular mechanics (MM) and molecular dynamics (MD) simulations were carried out to obtain the reasonable three dimensional (3D) structure of α-phosphomannomutase1. In the MM simulations, the system was governed by conjugate gradient method with Polak-Ribiere algorithm until the convergent criticism of the complex reach to 1×10^{-3} kcal mol^{-1} $Å^{-1}$. In the MD simulations, 500 ps simulations were carried out at constant temperature 298 K. And then, based on the structure obtained by MM and MD simulations, we used the affinity method to obtain the complex structure of α-phosphomannomutase1 and D-mannose 6-phosphate, in which D-mannose6-phosphate is swept into the active site upon cap closure. All the calculations mentioned above were carried out by using the Insight II software package developed by Accelrys [19]. The extensible and systematic force field (ESFF) [20] all-atom force field was used for the MD simulations.

Density functional theory calculations

All geometries and energies were computed using the DFT method with B3LYP functional [21–24] as implemented in the Gaussian03 program package [25]. 6–311G basis set was used for the geometry optimizations. On the basis of these geometries, single-point calculations on the larger basis set 6–311++G (2d,2p) were performed to obtain more accurate energies. Solvation energies were added to single-point calculations using the conductor-lick solvation model COSMO at the B3LYP functional with 6–311++G (2d, 2p) level. In these models, a cavity around the system is surrounded by a polarizable dielectric continuum. The dielectric constant chosen is ε=4, as is known that the standard value is used to model the protein surroundings. For all the models, the dielectric constant of ε=4 was used, the effect of using other dielectric constants are investigated in the first step in the protonated state, and results were shown to be quite insensitive to the choice of the constants (see Table 1) [26–28]. Hessians were calculated to confirm the nature of the stationary points, and were also used for evaluation of zero-point vibrational effects at the B3LYP/6–311G level. The energies reported in this study include both salvation and zero-point effects [29, 30]. In the geometry optimizations, certain truncation atoms were kept frozen to the position of the complex structure of α-phosphomannomutase1 and D-mannose 6-phosphate. This approach was used to keep the various groups in place to

Table 1 Calculated barriers in the first step (kcal mol^{-1}) of the protonated state with different dielectric constants

	ε=4	ε=8	ε=80
Barriers	7.6	7.4	7.0

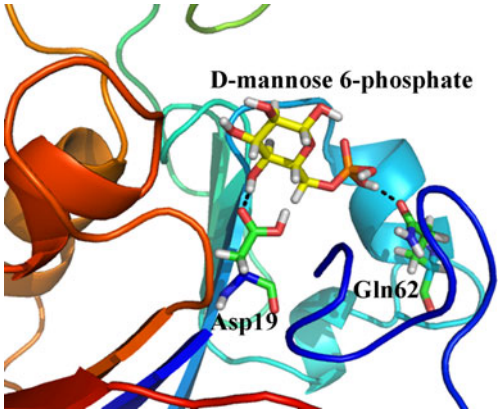

Fig. 1 The docking result of the complex structure

resemble the docked result as much as possible [26–29]. These fixed positions are indicated by arrows in the figures.

Quantum chemical models

Kinetic analysis experiments document the pH dependence of phosphomanno/phosphoglucomutase enzyme and illustrate the values of pK is 7.4 and 8.4 [14]. In order to make out the influence of the protonated state of phosphoryl group, we constructed two models: one keeps the phosphoryl group in protonated state, another one is in deprotonated state. As we mainly investigated that the process of the first phosphoryl transfers from Asp19 on the enzyme to bound substrate and produce a bisphosphorylated intermediate, the phosphoryl group of 6′ carbon remains in protonated state.

As always in quantum chemical studies, one has to make tradeoffs. On one hand, it is essential to choose the models to accurately represent the chemical situations [18]. In the present study, the models coordinates were taken from the complex α-phosphomannomutase1 and D-mannose 6-phosphate, and we had modeled the active site of α-phosphomannomutase1 in the following manner. **A.** The model of Asp19, which includes the side chain of the Asp19 and the phosphoryl group both in protonated/deprotonated states. **B.** The side chain of Gln62. **C.** The D-mannose 6-phosphate.

On the other hand, the models must be selected to test one or several reaction pathways and to find the transition states connection to the intermediates, a large number of calculations are usually required, and one has to keep the models at the right state.

Results and discussion

Docking study of α-phosphomannomutase1

With MM and MD simulations, the crystal structure of α-phosphomannomutase1 (PDB code 2FUC) was refined and the reasonable 3D structure of α-phosphomannomutase1 was obtained. We used D-mannose 6-phosphate as the substrate docking with the structure obtained above. Sivaggi *et al.* [12] reported that the active site of α-phosphomannomutase1, and based on the report, the binding pocket was constructed composed of 17 residues (Asp19, Asp21, Arg28, Gly53, Ser54, Lys58, Gln62, Arg132, Asn137, Pro140, Arg150, Ser188, Asp190, Lys198, Asn218, Glu219, Asn225). Sivaggi *et al.* [12] also revealed once the substrate is bound with the α-phosphomannomutase1, there is presumably a change in the conformation of the hinge region that pushes the substrate into the active site as the cap binds to core domain, and binding of the substrate would mitigate the repulsion of the cap and core domains, favoring cap closure. The structure of complex α-phosphomannomutase1 and D-mannose 6-phosphate which

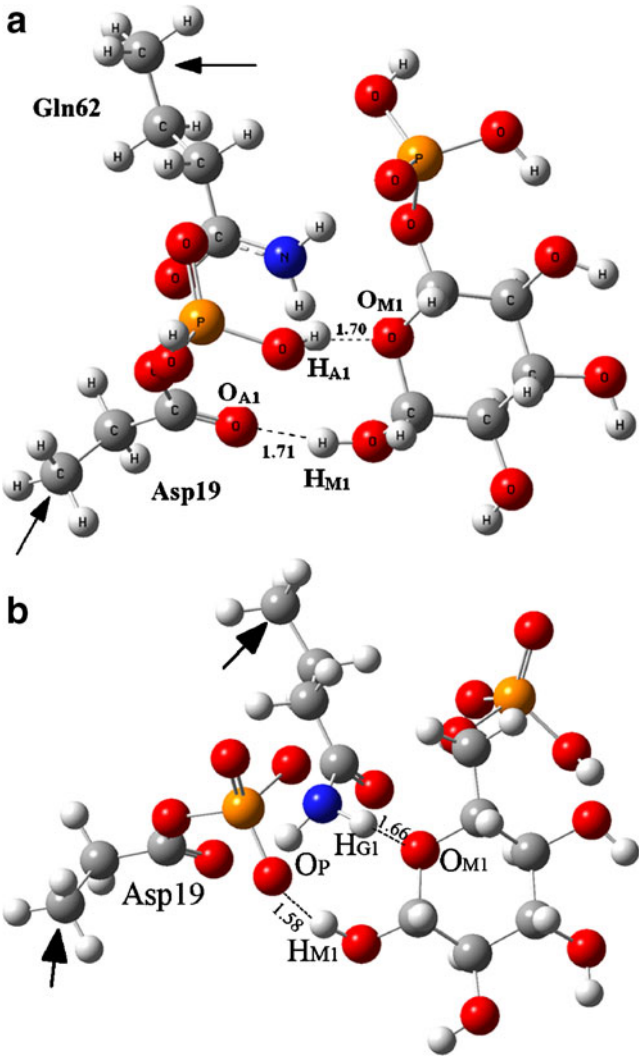

Fig. 2 Optimized structures of α-phosphomannomutase1 reactant models in protonated/deprotonated states. Arrows indicate frozen centers in the optimization: (**a**) the protonated state; (**b**) deprotonated state

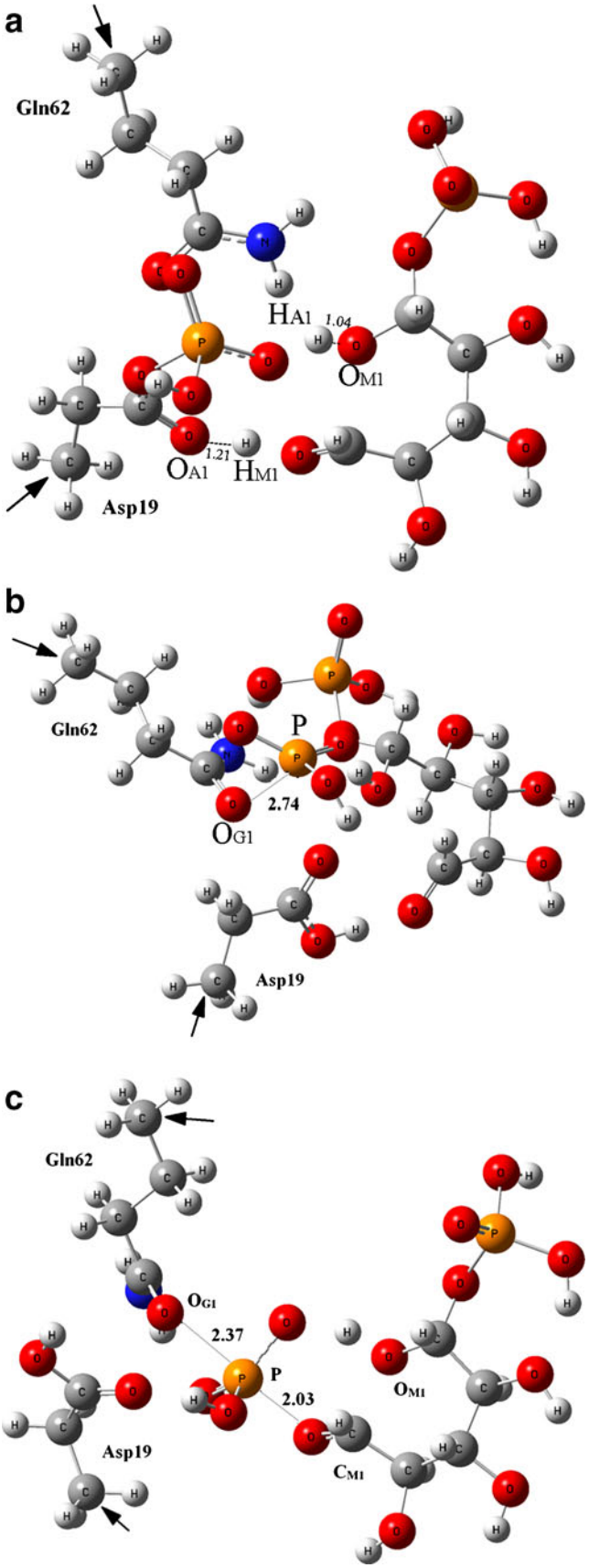

Fig. 3 Optimized structures in protonated state of (**a**) the transition-state structure of protons transfer between Asp19 and D-mannose 6-phosphate (TS1), (**b**) the transition state of the phosphoryl group departs from Asp19 close to Gln62 (TS2), (**c**) the transition state of the phosphoryl group transfers to the D-mannose 6-phosphate (TS3). Distances are given in Å

obtained by docking is displayed in Fig. 1. From Fig. 1, we can see that the substrate is swept into the active site in the complex α-phosphomannomutase1 and D-mannose 6-phosphate, and form the hydrogen bonds with Asp19 and Gln62. The total interaction energy of the α-phosphomannomutase1 and D-mannose 6-phosphate is −52.09 kcal mol^{-1}, the Van der Waals and electrostatic energies are −19.08 kcal mol^{-1} and −33.02 kcal mol^{-1}, respectively. Through interaction analysis, we know that Asp19 (−31.44 kcal mol^{-1}), Gly53 (−5.21 kcal mol^{-1}), Lys58 (−6.82 kcal mol^{-1}), Gln62 (−6.92 kcal mol^{-1}) and Arg132 (−6.11 kcal mol^{-1}) are important anchoring residues for α-phosphomannomutase1 and have main contribution to D-mannose 6-phosphate interaction, and Asp19 and Gln62 are the important amino acids. The docking results are in good agreement with the experiment results by Sivaggi *et al.* [12].

Reaction mechanism

In the present study, we discuss the reaction mechanism with the phosphoyl group in the protonated/deprotonated states. The two models in protonated/deprotonated states are shown in Fig. 2.

Protonated state

1. Protons transfer between the phosphoryl group of Asp19 and D-mannose 6-phosphate.

The first step (Step1) in the catalytic reaction of α-phosphomannomutase1 in protonated state is that the oxygen of the carboxyl in the Asp19 attacks the hydroxyl of the 1′ carbon in the D-mannose 6-phosphate; at the same time, a proton transfers from the phosphoryl group of the Asp19 to the oxygen of the ring in the D-mannose 6-phosphate.

In the model of reactant (R) (see Fig. 2a), the distance (dH_{M1}-O_{A1}) between the hydrogen (H_{M1}) in the hydroxyl of 1′ carbon in D-mannose 6-phosphate and the oxygen (O_{A1}) of the carboxyl in the Asp19 is 1.71 Å, and the distance (dH_{A1}-O_{M1}) between hydrogen (H_{A1}) in the phosphoryl group of the Asp19 and the oxygen (O_{M1}) of the ring is 1.70 Å. Then R overcomes the barrier energy 12.6 kcal mol^{-1} ($\Delta E = E_{TS1} - E_R$), and arrives at the transition state (TS) 1. Here, the dH_{M1}-O_{A1} decreases to 1.21 Å, and the dH_{A1}-O_{M1} decreases to 1.04 Å at the same

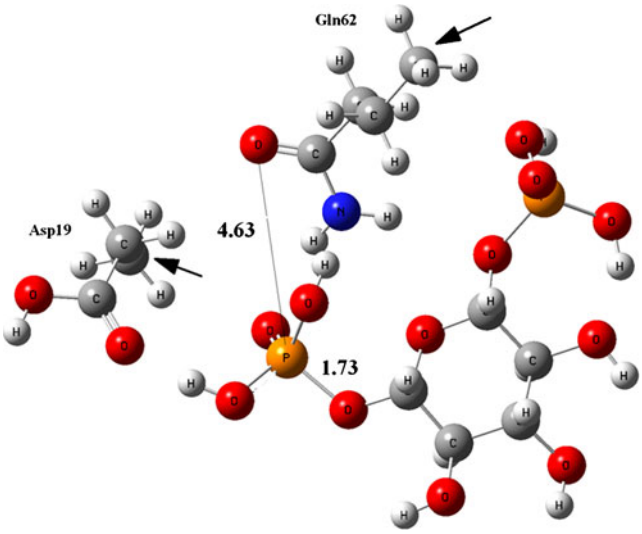

Fig. 4 Optimized structure of α-phosphomannomutase1 models in protonated states. Arrows indicate frozen centers in the optimization: the intermediate 3 with Mannose-1,6-(bis) phosphate

time. A proton transfer from D-mannose 6-phosphate to Asp19 is not evident from the optimized TS1 (shown in Fig. 3a). TS1 releases energy only 0.4 kcal mol^{-1} obtained intermediate (I) 1. We can see that the I1 is less steady, because the phosphoryl group as a result of losing a proton is in the state of activation. And dH_{M1}-O_{A1} and dH_{A1}-O_{M1} continue to decrease, which are 1.02 Å and 1.01 Å respectively. When H_{A1} transfers to O_{M1}, the distance (dC_{M1}-O_{M1}) between the 1'carbon (C_{M1}) of D-mannose 6-phosphate and O_{M1} increases to 2.38 Å, leading to the bond of the C_{M1}-O_{M1} broken. In the I1, the proton from D-mannose 6-phosphate transfers fully to Asp19. By contrasting the geometries of I1 and R, we can see that the bond length of the O-P in Asp19 increases, and the distance between phosphorus atom of Asp19 and the oxygen of carbonyl group in Gln62 decreases. The distance between the oxygen of the 1′ carbon in the D-mannose 6-phosphate and the phosphorus atom of the Asp19 is 4.26 Å in I1. It is impossible that the phosphoryl group transfers to the D-mannose 6-phosphate directly, as the distance between them is quite far away, the process needs a residue which can help to complete this transfer process of the phosphoryl group.

2. The phosphoryl group departs from Asp19 close to Gln62.

The next step (Step2) in the proposed mechanism of protonated state is that the phosphoryl group departs from Asp19 and moves close to Gln62. In this process, the bond of the O-P in the Asp19 is broken, and this will create the phosphoryl radical, and then the phosphoryl radical close to Gln62.

In Step1, the phosphoryl group is attacked by the O_{M1}, then it loses a proton, the phosphoryl group is in the state of activated. In the model of I1, the distance (dO_{G1}-P) between the oxygen (O_{G1}) of carbonyl group in Gln62 and the phosphorus (P) atom of Asp19 is 3.66 Å. The I1 overcomes the barrier energy 18.1 kcal mol^{-1} ($\Delta E = E_{TS2} - E_{I1}$), and arrives to the TS2 (shown in Fig. 3b). Here, the dO_{G1}-P decreases to 2.74 Å. The activated phosphoryl moves to the O_{G1} in order to stabilize it. TS2 releases energy 28.8 kcal mol^{-1} obtained I2, therefore the process is thermodynamically more favorable. The reaction energy of step2 is −10.7 kcal mol^{-1}. The dO_{G1}-P continues to decrease to 1.91 Å in I2. Although the dO_{G1}-P is longer than the standard bond length of the R, 1.76 Å, it should be noted that Gln62 can stabilize the phosphoryl group which departs from the Asp19. The phosphoryl group interacts with Asp19 through a hydrogen bond which can help to stabilize the structure. Because the phosphoryl group interacts with the enzyme in weak interaction, the group is less steady than R, therefore it can continue transfer to D-mannose 6-phosphate.

3. The phosphoryl group transfers D-mannose 6-phosphate.

The third step (Step3) in the proposed mechanism in protonated state is that the oxygen of the phosphoryl group attacks the hydroxyl of the D-mannose 6-phosphate, at last the phosphoryl group transfers to the carbonyl group of 1' carbon in the D-mannose 6-phosphate.

In this step, I2 overcomes the barrier energy 16.1 kcal mol^{-1} ($\Delta E = E_{TS3} - E_{I2}$), and arrives to the TS3 (shown in Fig. 3c). The phosphoryl group obtains a proton which it loses in Step1, and the O_{M1} tends to form a single bond with C_{M1} in the D-mannose 6-phosphate, which breaks in Step1. In TS3, we can see that the activated phosphoryl, which loses a proton in Step1, is apart from the Gln62 and moves towards to the carbonyl group of 1′ carbon in the D-mannose 6-phosphate. And TS3 releases energy 27.2 kcal mol^{-1} obtained I3 (shown in Fig. 4). The reaction energy is -11.1 kcal mol^{-1}. It should be noted that there is a hydrogen bond forming

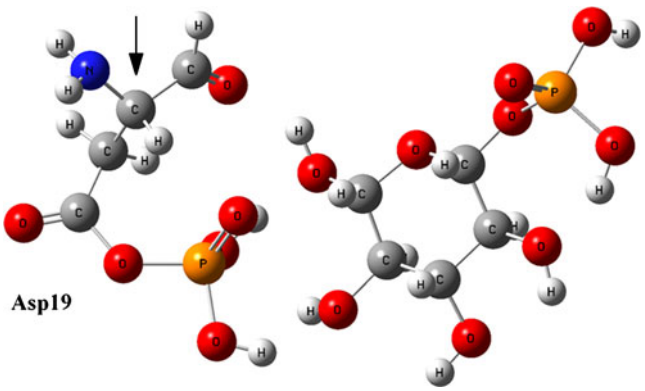

Fig. 5 Optimized structure of α-phosphomannomutase1 models in protonated states. Arrows indicate frozen centers in the optimization: contains only Asp19 and D-mannose 6-phosphate

between the oxygen of the phosphoryl group and proton which transfer in Step1, and this hydrogen bond is missing when the phosphoryl group transfers, resulting in the higher barrier. The bisphosphorylated intermediate is formed.

It should be noted that Gln62 is important for stabilizing the position of the D-mannose 6-phosphate. By contrasting the geometries of models that do not include Gln62 (see Fig. 5), we can see that D-mannose 6-phosphate rotates without Gln62, which deviates from the best position in the reaction. Gln62 also forms a hydrogen bond with D-mannose 6-phosphate, and in Step2 it interacts with the phosphoryl group stronger than before, that is to say the Gln62 could stabilize the position of the D-mannose 6-phosphate, when the substrate binds to the active site of α-phosphomannomutase1, and also can stabilize the phosphoryl group in the pathway of the reaction.

Deprotonated state

1. Protons transfer between the phosphoryl group, Gln62 and D-mannose 6-phosphate.

The first step (Step1') in the catalytic reaction of α-phosphomannomutase1 in deprotonated state is that the

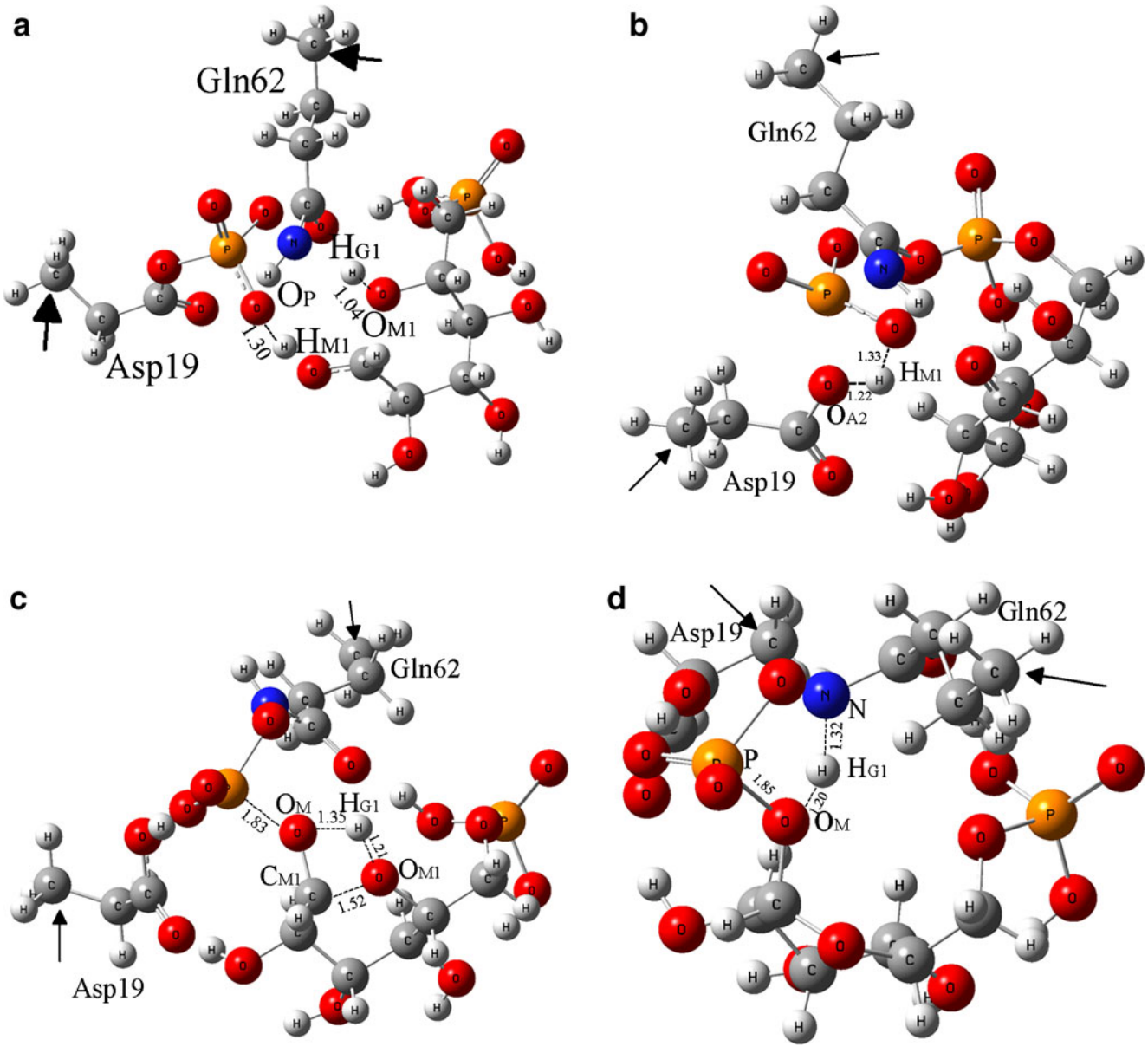

Fig. 6 Optimized structures in deprotonated state of (**a**) the transition-state structure of protons transfer between the phosphoryl group, Gln62 and D-mannose6-phosphate, (TS1'), (**b**) the transition state of proton transfers in phospho-Asp19 (TS2'), (**c**) the transition state of proton transfers in D-mannose 6-phosphate (TS3'). (**d**) the transition state of proton transfers from D-mannose 6-phosphate to Gln62 (TS4'). Distances are given in Å

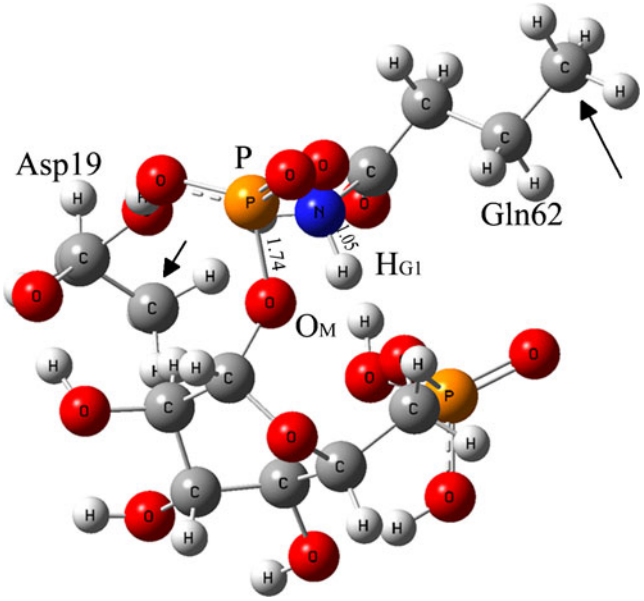

Fig. 7 Optimized structures of α-phosphomannomutase1 models in deprotonated states. Arrows indicate frozen centers in the optimization the intermediate 4' with Mannose-1,6-(bis) phosphate

oxygen of the phosphoryl group in the Asp19 attacks the hydroxyl of the 1' carbon in the D-mannose 6-phosphate; at the same time, a proton transfers from the amino of Gln62 to the oxygen of the ring in the D-mannose 6-phosphate.

In the model of R' (shown in Fig. 2b), the distance (dH_{M1}-O_P) between the hydroxyl hydrogen (H_{M1}) of 1' carbon in D-mannose 6-phosphate and oxygen (O_P) of the phosphoryl group is 1.58 Å, and the distance (dH_{G1}-O_{M1}) between the amino hydrogen (H_{G1}) of Gln62 and the oxygen (O_{M1}) of the ring is 1.66 Å. Then R' overcomes the barrier energy 7.6 kcal mol^{-1}, and arrives to the TS1' (see Fig. 6a). Here, the dH_{M1}-O_P decreases to 1.30 Å, and the dH_{G1}-O_{M1} decreases to 1.04 Å at the same time. A proton transfers from D-mannose 6-phosphate to phosphoryl is not evident from the optimized TS1'. TS1' releases energy 4.61 kcal mol^{-1} obtained I1'. And dH_{M1}-O_P and dH_{G1}-O_{M1} continue to decrease, which are both to 0.99 Å. When H_{G1} transfers to O_{M1}, the distance (dC_{M1}-O_{M1}) between the 1'carbon (C_{M1}) of D-mannose 6-phosphate and O_{M1} increases to 2.37 Å, leading to the bond of the C_{M1}-O_{M1} being broken.

2. Proton transfers in phospho-Asp19.

The next step (Step2') is that the proton obtained from D-mannose 6-phosphate transfers from phosphoryl group to carboxyl of the Asp19.

In the model of I1', the distance (dH_{M1}-O_{A2}) between (H_{M1}) and the carboxyl oxygen (O_{A2}) of Asp19 is 3.17 Å, Then I1' overcomes the barrier energy 26.81 kcal mol^{-1}, and arrives at the TS2' (see Fig. 6b). Here, the dH_{M1}-O_{A2} decreases to 1.22 Å. A proton transfer from O_P to Asp19 changes the protonated state of Asp19 resulting in the high barrier. TS2' releases energy 5.91 kcal mol^{-1} obtained I2'. And dH_{M1}-O_{A2} continues to decrease, which are 1.00 Å. When H_{M1} transfers to O_{A2}, the distance (dP-O_{A2}) between P and O_{A2} increases to 2.34 Å, leading to the bond of the P-O_{A2} being broken. In the I2', the H_{M1} transfers fully to Asp19, and phosphoryl group departs from Asp19. The distance between P and the amino nitrogen (N) of Gln62 decreases. The N tends to interact with phosphoryl group oxygen with the weak interaction, and the Gln62 may help to stabilize the phsosphoryl radical.

3. Proton transfesrs in D-mannose 6-phosphate.

The next step (Step3') is that the proton obtained from Gln62 transfers from O_{M1} to the oxygen of the 1' carbon in the D-mannose 6-phosphate.

In the model of I2', the distance (dH_{G1}-O_M) between H_{G1} and the oxygen of the 1' carbon (O_M) is 3.08 Å, Then I2' overcomes the barrier energy 5.85 kcal mol^{-1}, and

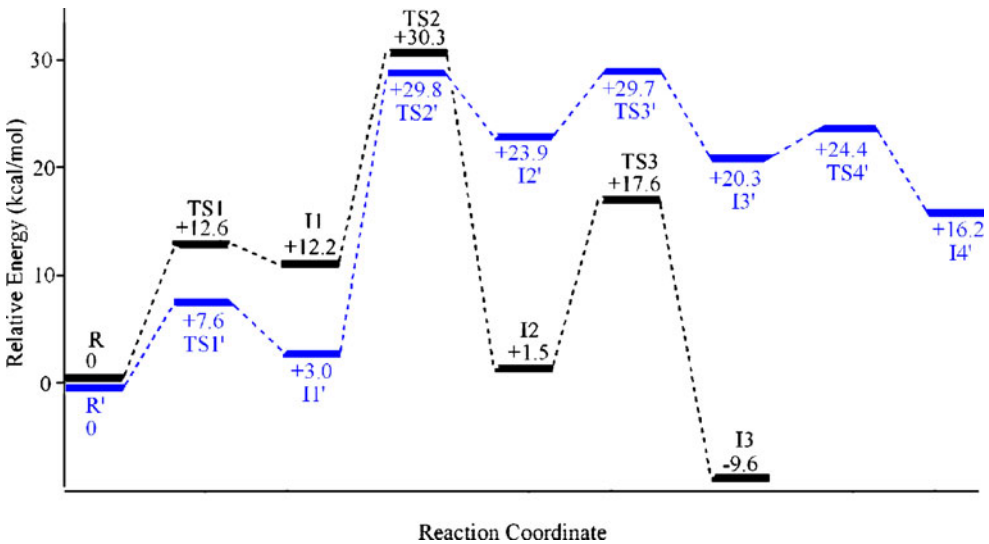

Fig. 8 Calculated potential energy surface for the reaction of α-phosphomannomutase1 as in protonated (color in black) /deprotonated (color in blue) states

arrives to the TS3' (see Fig. 6c). Here, the dH_{G1}-O_M decreases to 1.35 Å, at the same time dC_{M1}-O_{M1} decreases to 1.52 Å, and bond of C_{M1}-O_{M1} tends to reconnect. It should be noted that dP-O_M is 1.83 Å, and the phosphoryl group tends to connect to the D-mannose 6-phosphate. TS3' releases energy 9.49 kcal mol^{-1} obtained I3'. And dH_{G1}-O_M continues to decrease, which are 0.98 Å. When H_{G1} transfers to O_M, the dC_{M1}-O_{M1} decreases to 1.39 Å, leading to the bond of the C_{M1}-O_{M1} being reformed. In the I3', the H_{G1} transfers fully to O_M, the dP-O_M increases to 1.99 Å and phosphoryl group still exists in radical form. And the amino of the Gln62 as a result of losing a proton, is a less steady state.

4. Proton transfers from D-mannose 6-phosphate to Gln62.

The next step (Step4') is that the proton obtained from Gln62 transfers from D-mannose 6-phosphate back to Gln62.

In the model of I3', the distance (dH_{G1}-N) between H_{G1} and the amino nitrogen (N) is 3.33 Å, Then I3' overcomes the barrier energy 4.19 kcal mol^{-1}, and arrives at the TS4' (see Fig. 6d). Here, the dH_{G1}-N decreases to 1.32 Å, at the same time dP-O_M decreases to 1.85 Å, and bond of P-O_M tends to connect. TS4' releases energy 8.20 kcal mol^{-1} obtained I4' (shown in Fig. 7). dH_{G1}-N continues to decrease, which are 1.05 Å. When H_{G1} transfers back to N, the dP-O_M decreases to 1.74 Å, leading to the bond of the P-O_M fully forming. The bisphosphorylated intermediate is formed.

Potential energy surface

Based on the calculations, the different protonated states of phosphoryl group are provided with different reaction mechanism in the following points. The Asp19 as nucleophile obtains the proton from the D-mannose 6-phosphate in different pathway: in protonated state, Asp19 gains the proton directly, the proton transfers from the 1' carbon hydroxyl to the carboxyl oxygen of the Asp19; but in deprotonated state, the proton first transfers to the oxygen of the phosphoryl group, then to oxygen of the bond O-P in the Asp19. The oxygen of the ring in the D-mannose 6-phosphate must obtain a proton as a result of the step1 D-mannose 6-phosphate losing a hydrogen atom, but the hydrogen source is different: in protonated state, because the phosphoryl group is protonated and its hydrogen atom forms a hydrogen bond with the oxygen of the ring, the oxygen atom directly gains a hydrogen atom from the phosphoryl group giving rise to the activation state of phosphoryl group; but in deprotonated state, the oxygen atom obtains the hydrogen from the amino group of Gln62, and forms amino radical. The hydrogen atom which was obtained by oxygen ring in the D-mannose 6-phosphate transfers back to the original site in a different pathway: in protonated state, the hydrogen atom directly transfers back; but in deprotonated state, the process of the hydrogen transferring back is proposed through the intermediate 3', which a hydrogen atom connected back to the oxygen of 1' carbon.

The calculated potential energy surface (PES) for the reaction of the substrate change from D-mannose 6-phosphate to mannose-1,6-(bis) phosphate intermediate both for protonated/deprotonated states is presented in Fig. 8. From the PES, we can see that mannose-1, 6-(bis) phosphate intermediate is more stably bound with α-phosphomannomutase1 in the protonated state, and the inhibition is stronger than in the deprotonated state. It should be noted that if the mannose-1,6-(bis) phosphate intermediate serves as the substrate, the barriers in the pathway of the deprotonted state are 8.2 kcal mol^{-1}, 9.4 kcal mol^{-1}, 5.9 kcal mol^{-1} and 4.6 kcal mol^{-1}, they are lower than the protonted state. In other words, the deprotonated state is more suited for the interconversion reaction which takes place from the bis-phosphate intermediate to the product, Naught *et al*. [14] have defined the pK's of 7.4 and 8.4 from the substrate glucose-6-phosphate. The phosphoryl group is deprotonated in this range of pH, that is to say the deprotonated state is more suitable for the reaction. Our calculation well accorded with the experimental results by Naught *et al*. [14].

Conclusions

In the present study, the reaction mechanism of α-phosphomannomutase1 is proposed in both protonated/deprotonated states, and investigated with the quantum chemical method. By considering the experimental fact [12] and our calculated results, two models are chosen as the more favorable model to investigate the reaction mechanism. Based on the calculations, the different protonated states of phosphoryl group are provided with different reaction mechanisms. And the process of the phosphoryl group transferred from Asp19 to the mannose 6-phosphate is in different steps in the two states, but both are coupled with the protons transfer. From the PES calculations, we can see that mannose-1, 6-(bis) phosphate intermediate is more stably bound with α-phosphomannomutase1 in the protonated state, and the inhibition is stronger than in the deprotonated state, which is well accorded with the experimental results by Naught *et al*. [14]. In addition, Asp19 as a nucleophile plays a vital role in the process of reaction mechanism, which is consistent with the experimental results by Silvaggi *et al*. [12]. By considering the Gln62 at the active site, it should be noted that Gln62 is another important residue, which could help to stabilize the phosphoryl group and the substrate.

Acknowledgments This work is supported by the Natural Science Foundation of China, Key Projects in the National Science & Technology Pillar Program, Specialized Research Fund for the Doctoral Program of Higher Education, and Specialized Fund for the Basic Research of Jilin University (Grant Nos. 20903045, 20573042, 2006BAE03B01, 20070183046, and 200810018).

References

1. Westphal V, Enns GM, McCracken MF, Freeze HH (2001) Functional analysis of novel mutations in a congenital disorder of glycosylation Ia patient with mixed Asian ancestry. Mol Genet Metab 73:71–76
2. Pirard M, Achouri Y, Collet JF, Schollen E, Matthijs G, Van Schaftingen E (1999) Kinetic properties and tissular distribution of mammalian phosphomannomutase isozymes. Biochem J 339:201–207
3. Matthijs G, Schollen E, Pardon E, Veiga-Da-Cunha M, Jaeken J, Cassiman JJ, van Schaftingen E (1997) Mutations in PMM2, a phosphomannomutase gene on chromosome 16p13, in carbohydrate-deficient glycoprotein type I syndrome (Jaeken syndrome). Nat Genet 16:88–92
4. Matthijs G, Schollen E, Van Schaftingen E, Cassiman JJ, Jaeken J (1998) Lack of homozygotes for the most frequent disease allele in carbohydrate-deficient glycoprotein syndrome type 1A. Am J Hum Genet 62:542–550
5. Neumann LM, von Moers A, Kunze J, Blankenstein O, Marquardt T (2003) Congenital disorder of glycosylation type 1a in a macrosomic 16-month-old boy with an atypical phenotype and homozygosity of the N216I mutation. Eur J Pediatr 162:710–713
6. Van Schaftingen E, Jaeken J (1995) Phosphomannomutase deficiency is a cause of carbohydrate-deficient glycoprotein syndrome type I. FEBS Lett 377:318–320
7. Westphal V, Srikrishna G, Freeze HH (2000) Congenital disorders of glycosylation: have you encountered them? Genet Med 2:329–337
8. Marquardt T, Hasilik M, Niehues R, Herting M, Muntau A, Holzbach U (1997) Mannose therapy in carbohydrate-deficient glycoprotein syndrome type I: first results from a German multicenter study. Amino Acids 12:389
9. Kristiansson B, Borulf S, Conradi N, Erlanson-Albertsson C, Ryd W, Stibler H (1998) Intestinal, pancreatic and hepatic involvement in carbohydrate-deficient glycoprotein syndrome type I. J Pediatr Gastroenterol Nutr 27:23–29
10. Carchon H, van Schaftingen E, Matthijs G, Jaeken J (1999) Carbohydrate-deficient glycoprotein syndrome type IA (phosphomannomutase-deficiency). Biochim Biophys Acta 1455:155–165
11. Heykants L, Schollen E, Grünewald S, Matthijs G (2001) Identification and localization of two mouse phosphomannomutase genes, Pmm1 and Pmm2. Gene 270:53–59
12. Silvaggi NR, Zhang C, Lu Z, Dai J, Dunaway-Mariano D, Allen KN (2006) The X-ray crystal structures of human alpha-phosphomannomutase 1 reveal the structural basis of congenital disorder of glycosylation type 1a. J Biol Chem 281:14918–14926
13. Dai JB, Liu Y, Ray WJ Jr, Konno M (1992) The crystal structure of muscle phosphoglucomutase refined at 2.7-angstrom resolution. J Biol Chem 267:6322–6337
14. Naught LE, Tipton PA (2001) Kinetic mechanism and pH dependence of the kinetic parameters of Pseudomonas aeruginosa phosphomannomutase / phosphoglucomutase. Arch Biochem Biophys 396:111–118
15. Regni C, Schramm AM, Beamer LJ (2006) The reaction of phosphohexomutase from Pseudomonas aeruginosa: structural insights into a simple processive enzyme. J Biol Chem 281:15564–15571
16. Cheng Y, Zhang Y, McCammon JA (2005) How does the cAMP-dependent protein kinase catalyze the phosphorylation reaction: an ab initio QM/MM study. J Am Chem Soc 127:1553–1562
17. Corminboeuf C, Hu P, Tuckerman ME, Zhang Y (2006) Unexpected deacetylation mechanism suggested by a density functional theory QM/MM study of histone-deacetylase-like protein. J Am Chem Soc 128:4530–4531
18. Chen SL, Marino T, Fang WH, Russo N, Himo F (2008) Peptide hydrolysis by the binuclear zinc enzyme aminopeptidase from Aeromonas proteolytica: a density functional theory study. J Phys Chem B 112:2494–2500
19. Insight II User Guide, Accelrys Inc, San Diego, 2000
20. Discover3 User Guide, Accelrys Inc, San Diego, 2000
21. Becke AD (1993) Density-functional thermochemistry. III. The role of exact exchange. J Chem Phys 98:5648–5652
22. Becke AD (1992) Density-functional thermochemistry. I. The effect of the exchange-only gradient correction. J Chem Phys 96:2155–2160
23. Becke AD (1992) Density-functional thermochemistry. II. The effect of the Perdew–Wang generalized-gradient correlation correction. J Chem Phys 97:9173–9177
24. Lee C, Yang W, Parr RG (1988) Development of the Colle-Salvetti correlation-energy formula into a functional of the electron density. Phys Rev B 37:785–789
25. Gaussian 03, Revision A.1, Gaussian Inc, Pittsburgh PA, 2003
26. Velichkova P, Himo F (2006) Theoretical study of the methyl transfer in guanidinoacetate methyltransferase. J Phys Chem B 110:16–19
27. Velichkova P, Himo F (2005) Methyl transfer in glycine N-methyltransferase. A theoretical study. J Phys Chem B 109:8216–8219
28. Hopmann KH, Himo F (2008) Cyanolysis and azidolysis of epoxides by haloalcohol dehalogenase: theoretical study of the reaction mechanism and origins of regioselectivity. Biochemistry 47:4973–4982
29. Himo F (2006) Quantum chemical modeling of enzyme active sites and reaction mechanisms. Theor Chem Acc 116:232–240
30. Curtiss LA, Raghavachari K, Redfern PC, Pople JA (1997) Assessment of Gaussian-2 and density functional theories for the computation of enthalpies of formation. J Chem Phys 106:1063–1079